1-1-1964

Power spectral density measurements in the Iowa State University UTR-10 reactor

Stamatis Nicholas Paleocrassas
Iowa State University

POWER SPECTRAL DENSITY MEASUREMENTS IN THE IOWA STATE UNIVERSITY UTR-10 REACTOR

by

Stamatis Nicholas Paleocrassas

A Thesis Submitted to the
Graduate Faculty in Partial Fulfillment of
The Requirements for the Degree of
MASTER OF SCIENCE

Major Subject: Nuclear Engineering

Iowa State University
Of Science and Technology
Ames, Iowa

1964

TABLE OF CONTENTS

I. SUMMARY

The present investigation utilizes a very important statistical property, namely the power spectral density of the random variation of the neutron flux, which evaluates some important parameters of the Iowa State University UTR-10 nuclear reactor. Using the same property an attempt was also made to compare the neutron flux variation between two different locations inside the reactor with the system in the critical as well as in the subcritical state.

The "power spectral density" can be loosely defined as a measure of the total average power in a given frequency band width of a random signal.

The UTR-10 reactor, as a linear system, was characterized by its power spectra response to a random disturbance whose power spectral density was known. The random disturbance was provided by a plutonium-beryllium neutron source placed between the two subcores of the reactor. Thus, the magnitude of the transfer function of the reactor was obtained over a certain frequency domain. The span of this frequency domain was chosen to be from 0.1 to 10^3 cps, within which the characteristic modes of the desired reactor parameters were expected to lie. The desired parameters in the present investigation were the effective multiplication constant

(Keff) and the ratio (β/ℓ) where β is the delayed neutron fraction and ℓ the effective neutron lifetime. The expression which relates the parameters to the source transfer function of the subcritical reactor is given by

$$|H_r(\omega)|^2 = \frac{1}{\omega^2 + [\frac{1-Keff(1-\beta)}{\ell}]^2} \qquad (1)$$

From this expression it is clear that the quantity $[\frac{1-Keff(1-\beta)}{\ell}]$ is given by the corner frequency co-ordinate of the specific transfer function. Data describing characteristic Bode curves were obtained for the reactor critical and subcritical with the detecting instrument placed at two different locations inside the reactor. Finally, the data were fitted by a least square technique into a more detailed form of Equation (1) in order to obtain the corner frequency and thereby the quantity $[\frac{1-Keff(1-\beta)}{\ell}]$.

Finally, part of this study was to investigate a special detecting technique to be used for the detection of the neutron flux when the reactor is quite subcritical. The necessity of such a technique has been indicated by the failure of ionization chambers to detect weak neutron flux signals.

II. INTRODUCTION

> By simply analyzing the random fluctuations in the power level of a reactor one can obtain, free of charge, a continuous report on reactor operating variables which can be of great value in guiding the decisions of the operator. J. A. Thie (13)

When a broad band of random noise is applied to the imput of some physical device the statistical properties of the output of the system are often of interest. For example, in the case of a nuclear reactor, the random fluctuations of the neutron level which are generated by an inherent random reactivity input can be analyzed to obtain information about the system. Two of the most important statistical properties which are involved in the analysis of neutron level fluctuations are the autocorrelation function and the power spectral density. The former is considered as a measure of the dependence of values of a random output separated by a fixed time interval, while the later is defined as the limit of the total average power in a given bandwidth of frequencies divided by the bandwidth as the bandwidth approaches zero.

The power spectral density can be determined experimentally by analyzing the random signal in question with respect to different frequencies. The result can then be interpreted by means of a "Bode" plot. If a nuclear reactor is considered as a linear system then the output power spectral density is expressed in terms of the square

modulus of the transfer function and the power spectral density of the driving function. Thus, if the input power spectral density is known, the measured output power spectral density can be used to obtain the magnitude of the system's transfer function.

The spatially independent transfer function for a subcritical reactor has been shown to be a function of the effective multiplication constant, Keff, of the system (14). Thus, it is possible to obtain the shutdown margin of the system from power spectral density measurements.

III. LITERATURE SURVEY

Although the technique for collecting and interpreting data in reactor noise analysis is not well known, its use for obtaining information about the reactor's parameters is becoming very popular.

The use of reactor noise analysis, in general, has evolved since the theory for analysing functions of time with a random behavior has been fully developed. Schuster (11) is believed to be the first to investigate random functions, and he is well known for his "periodgram" method of analysis. The use of random techniques in reactor analysis started with Moore (7), while Rice's analytical studies contributed to the formulation of pile noise (9). Griffin and Lundholm (4) have done systematic measurements of power spectral densities for critical reactors. Recent studies and detailed descriptions of newly developed measuring techniques have been summarized in a book by Thie (12). For a more recent reference on noise analysis in nuclear systems, one ought to refer to the symposium on reactor kinetics which took place at the University of Florida during the current year. Papers were presented concerning various investigations of nuclear systems using noise analysis techniques such as auto- and cross-correlations as well as power and cross spectral densities. Analog and digital computer methods were used for the measurements.

In contrast with the above numerous investigations one can find only a few systematic efforts involved with shutdown reactivity measurements. Uhrig (14) has made an intensive study concerning the characteristic of subcritical assemblies. He concluded that the dynamic characteristics are dependent on the degree of departure from criticality as well as on neutron lifetime. Starting from the general non-linear form of the neutron kinetic equation and after making the necessary assumptions to fit the situation, he concluded that the frequency dependent power spectral density ratio of output to input for the reactor is given by the expression

$$\left|\frac{N(f)}{S(f)}\right|^2 = \frac{1}{\omega^2 + \left[\frac{(1-\beta)K_{eff}-1}{\ell}\right]^2} \qquad (2)$$

where S(f), the white-noise spectrum of source neutrons, is constant. Badgley (1) utilized the above relationship by constanting power spectral density measurements in the subcritical region for the University of Florida Training reactor.

Nomura and Goto[1] obtained subcritical measurements Using the power spectral density technique on the TTR-I

---

[1]Nomura, T. and Goto, S., Japan Atomic Energy Research Institute. Kenetic studies of nuclear reactors by statistical methods. Private communication to Dr. Richard Danofsky, Assistant Professor of Nuclear Engineering, Iowa State University, Ames, Iowa. 1964.

reactor (swimming pool type). They used a two-energy group subcritical reactor model developed by Nomura. His method, although developed independently, is quite similar to Uhrig's as far as the determination of subcritical reactivity is concerned. However, Uhrig ignored β, the delayed neutron fraction, compared to one and thus he obtained $\frac{1-K}{\ell}$ for large degrees of subcriticality instead of $\frac{\beta}{\ell}(1-\frac{K-1}{K\beta})$ as obtained by Nomura.

After investigation most of the above techniques for shutdown reactivity measurements, it may be concluded that they are similar as far as the interpretation of the experimental results are concerned, and they differ only with respect to the method used to obtain the data. For example, Yamada[1] recorded the output signal from the reactor after it was initially amplified, on tape with an FM magnetic tape recorder and re-recorded it to permit playback at 2, 8, 16, 32 times the original recording speed. Thus, speed up of the tape permitted playback of thirty minutes of data in one minute. Schultz (10) used a hydrogen-filled ion chamber for detecting the signal, and developed a special very low noise preamplifier for obtaining a good size signal.

---

[1]Yamada, S., Japan Atomic Energy Research Institute. Kinetic studies of nuclear reactors by statistical methods. Private communication to Dr. Richard Danofsky, Assistant Professor of Nuclear Engineering, Iowa State University, Ames, Iowa. 1964.

Finally, the work done up to date at Iowa State University Consists of Leribaux's (6) general study on stochastic processes in coupled reactor cores, and Danofsky's (3) random noise analysis in the Iowa State University UTR-10 reactor. Both of these investigations included power spectral density measurements with the reactor critical. Thus, it is believed the present study is the first investigation conducted on the UTR-10 reactor which involves subcritical measurements.

IV. THEORY

A. Basic Analytical Relationship Relating Input and Output Power Spectral Densities

The basic relationship between the input and output power spectral densities for a linear system will be formally reviewed in this section. The presentation here follows that given by Lee (5).

The autocorrelation function of a random signal $F(t)$ is defined as

$$\varphi_{oo}(\tau) = \lim_{T\to\infty} \frac{1}{2T}\int_{-T}^{T} F_o(t)F_o(t+\tau)dt, \qquad (3)$$

where τ is a variable time delay.

When a unit impulse excites a linear system, the output response, which is known as the "impulse response", characterizes the system. That is, the output of the linear system for any input function can be expressed in terms of the "impulse response" function and the input by means of the convolution integral.

Consider a linear system which is characterized by an "impulse response" $H(t)$, and is subjected to an input $F_i(t)$. The output of $F_o(t)$ can be expressed as

$$F_o(t) = \int_{-\infty}^{\infty} H(v)F_i(t-v)dv \ . \qquad (4)$$

The autocorrelation function of the system's output can then be expressed as

$$\varphi_{oo}(\tau) = \lim_{T\to\infty} \frac{1}{2T}\int_{-T}^{T} \left\{ \int_{-\infty}^{\infty} H(v)F_i(t-v)dv \int_{-\infty}^{\infty} H(\sigma)F_i(t+\tau-\sigma)d\sigma \right\} dt, \quad (5)$$

by utilizing Equation (3) for $F_o(t)$ and

$$\int_{-\infty}^{\infty} H(\sigma)F_i(t+\tau-\sigma)d\tau, \text{ for } F_o(t+\tau). \quad (6)$$

The order of integration of Equation (5) may be interchanged to obtain

$$\varphi_{oo}(\tau) = \left\{ \int_{-\infty}^{\infty} H(v)dv \int_{-\infty}^{\infty} H(\sigma)d\sigma \left[\lim_{T\to\infty} \frac{1}{2T} \int_{-T}^{T} F_i(t-v)F_i(t+\tau-\sigma)dt \right] \right\}. \quad (7)$$

The expression in the brackets is the autocorrelation of the input random signal, $\varphi_{ii}(v+\tau-\sigma)$. Thus, Equation (7) can be written as

$$\varphi_{oo}(\tau) = \int_{-\infty}^{\infty} H(v)dv \int_{-\infty}^{\infty} H(\sigma)\, \varphi_{ii}(v+\tau-\sigma)d\sigma. \quad (8)$$

The power spectral density of the random signal $F_o(t)$, $\Phi_{oo}(\omega)$, is defined as the Fourier Transform of $\varphi_{oo}(\tau)$. From the definition of the Fourier Transform it follows that

$$\Phi_{oo}(\omega) = \frac{1}{2\pi}\int_{-\infty}^{\infty} \varphi_{oo}(\tau)e^{-j\omega\tau}d\tau. \quad (9)$$

Substitution of Equation (8) for $\varphi_{oo}(\tau)$ yields

$$\Phi_{oo}(\omega) = \frac{1}{2\pi}\int_{-\infty}^{\infty} e^{-j\omega\tau} \left\{ \int_{-\infty}^{\infty} H(v)dv \int_{-\infty}^{\infty} H(\sigma)\, \varphi_{ii}(\tau+v-\sigma)d\sigma \right\} d\tau. \quad (10)$$

With the change of variable, $\mu = (\tau+v-\sigma)$, Equation (10) becomes

$$\Phi_{oo}(\omega) = \frac{1}{2\pi}\int_{-\infty}^{\infty} e^{-j\omega(\mu+\sigma-\nu)}\left[\int_{-\infty}^{\infty} H(\nu)d\nu \int_{-\infty}^{\infty} H(\sigma)\,\varphi_{ii}(\mu)d\sigma\right]d\mu. \quad (11)$$

An interchange of the order of integration yields

$$\Phi_{oo}(\omega) = \int_{-\infty}^{\infty} H(\nu)e^{j\omega\nu}d\nu \int_{-\infty}^{\infty} H(\sigma)e^{-j\omega\sigma}d\sigma\left[\frac{1}{2\pi}\int_{-\infty}^{\infty}\varphi_{ii}(\mu)e^{-j\omega\mu}d\mu\right]. \quad (12)$$

Assuming that $H(t) = H(t)$ for $t>0$ and $H(t) = 0$ for $t<0$, the limits of the first two integrals in Equation (11) become from 0 to ∞.

$$\Phi_{oo}(\omega) = \int_{0}^{\infty} H(\nu)e^{j\omega\nu}d\nu \int_{0}^{\infty} H(\sigma)e^{-j\omega\sigma}d\sigma\left[\frac{1}{2\pi}\int_{-\infty}^{\infty}\varphi_{ii}(\mu)e^{-j\omega\mu}d\mu\right]. \quad (13)$$

The first integral in Equation (13) is the frequency response function, $H(\omega)$, of the system and the second integral is its complex conjugate, $\overline{H}(\omega)$. The expression in the brackets represents the power spectral density of the random input to the linear system, $\Phi_{ii}(\omega)$. Equation (13) can, thus, be written as

$$\Phi_{oo}(\omega) = H(\omega)\overline{H}(\omega)\,\Phi_{ii}(\omega), \quad (14)$$

or

$$\Phi_{oo}(\omega) = |H(\omega)|^2\,\Phi_{ii}(\omega). \quad (15)$$

This is the fundamental analytical relationship used in the present investigation for the interpretation of the experimental results. However, due to the fact that in the system as a whole there are relatively uncorrelated noise contributions from the driving neutron

source and the instrumentation itself, the above relationship becomes a little more complex. Badgley and Uhrig (2) have represented the reactor and instrumentation with the block diagram shown in Figure 1. The power spectral density of the output of the system is then given as

$$\Phi_{oo}(\omega) = \Phi_{ii}(\omega)|H_R(j\omega)|^2 \, |H_M(j\omega)|^2 + \Phi_{nn}(\omega)|H_M(j\omega)|^2, \quad (16)$$

where:

$\Phi_{oo}(\omega)$ = Output power spectral density of the reactor and instrumentation

$\Phi_{ii}(\omega)$ = Power spectral density of the neutron source noise (white)

$\Phi_{nn}(\omega)$ = Power spectral density of the instrumentation noise

$H_R(j\omega)$ = Frequency response of the reactor

$H_M(j\omega)$ = Frequency response of the instrumentation.

Due to the fact that $\Phi_{nn}(\omega)$ and $\Phi_{ii}(\omega)$ are power spectral densities of uncorrelated random noise, they can be considered as constants up to very high frequencies. Thus, equation (16) can be corrected for the instrument frequency response by dividing each side by $|H_M(j\omega)|^2$. This yields

$$\frac{\Phi_{oo}(\omega)}{|H_M(j\omega)|^2} = \Phi_{ii}(\omega)|H_R(j\omega)|^2 + \Phi_{nn}(\omega), \quad (17)$$

or

Figure 1. Block diagram representation of the reactor and instrumentation

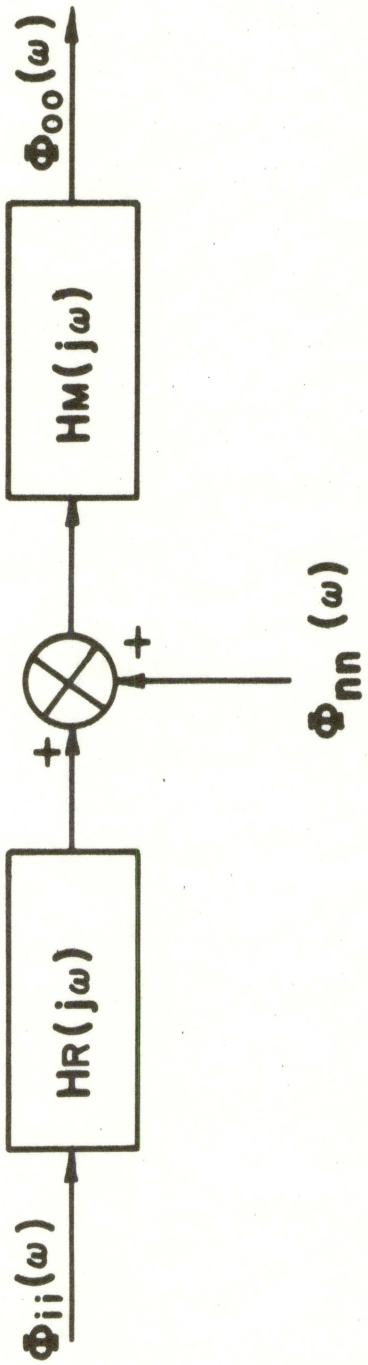
$\Phi_{oo}(\omega)$
HM(jω)
+
+
$\Phi_{nn}(\omega)$
HR(jω)
$\Phi_{ii}(\omega)$

$$\frac{\Phi_{oo}(\omega)}{|H_R(j\omega)|^2} = A + B|H_R(j\omega)|^2. \qquad (18)$$

Here, the constants A and B represent the power spectral densities of the instrument noise and input noise, respectively.

B. Derivation of the Open Loop Subcritical Reactor Transfer Function

The modulus of the open loop subcritical reactor transfer function which is to be used with the relationship between the power spectral densities of the input and output of the system is now derived. The UTR-10 reactor is a commercial version of the Argonne National Laboratory Argonaut type. The core configuration consists of two separate sub-cores of fuel regions embedded in graphite. Deionized light water, which serves as both moderator and coolant, is circulated through each fuel region. Each fuel region is subcritical when considered separately and the exchange of neutrons between the two regions makes the system critical. A reactivity coupling coefficient accounts for this reactivity exchange between the two sub-cores, and is a function of the distance between the regions.

The analytical model to be used next in order to describe the kinetic behavior of the reactor posesses the drawback that, in solving the time dependent thermal

neutron diffusion equation (with extraneous source term), it has been assumed that the spatial destribution of neutrons for the reactor is described by the fundamental eigenfunction. This, of course, calls for the assumption that Keff is very near the value of one. However, when a subcritical system is involved, the degree of departure from criticality is quite significant and the situation calls for questioning the accuracy of the theoretical model used for the interpretation of the experimental results. Regardless, though, of this drawback the model has been used extensively by investigators and it has yielded reasonably assurate results (2).

The kinetic equations which describe the dynamic behavior of the reactor, assuming one group of delayed neutrons and also that the flux distribution is described by the fundamental eigenfunction, can be written as

$$\frac{dN}{dt} = [K(1-\beta)-1]\frac{N}{\ell} + \lambda C + H, \tag{19}$$

and

$$\frac{dC}{dt} = \frac{\beta K N}{\ell} - \lambda C, \tag{20}$$

where N and C are the average neutron density and precursor concentration in the reactor respectively, β is the effective delayed neutron fraction, ℓ is the prompt neutron lifetime, λ is the average decay constant for the precursors, K is the effective reproduction constant, and H is the external driving source, in this case the input

from a Pu-Be neutron source.

In order to derive the transfer function of the reactor with respect to the source, it is assumed that the source fluctuates about some steady value. This is expressed as

$$H = H_o + H_1(t), \tag{21}$$

where H_o is the steady state source strength and $H_1(t)$ accounts for the time variations of the source. These source fluctuations affect the neutron density and precursors in such a manner that they also experience similar fluctuations according to

$$N = N_o + N_1(t), \tag{22}$$

and

$$C = C_o + C_1(t). \tag{23}$$

Substitution of Equations (21), (22), and (23) into Equations (19) and (20) yields

$$\frac{dN_1(t)}{dt} = [K(1-\beta)-1]\frac{N_1(t)}{\ell} + \lambda C_1(t) + H_1(t), \tag{24}$$

and

$$\frac{dC_1(t)}{dt} = \frac{\beta K N_1(t)}{\ell} - \lambda C_1(t), \tag{25}$$

respectively, after elimination of the time independent terms. To derive the source transfer function, $N_1(s)/H_1(s)$, in turn, the Laplace Transform of Equations (24) and (25) is obtained.

$$\frac{N_1(s)}{H_1(s)} = \frac{1}{s - \frac{[K(1-\beta)-1]}{\ell} - \frac{\lambda\beta K}{(s+\lambda)}} , \tag{26}$$

or

$$\frac{N_1(s)}{H_1(s)} = \frac{s + \lambda}{s^2 - \frac{[K(1-\beta)-1]}{\ell} s + \frac{(1-K)\lambda}{\ell}} . \tag{27}$$

Here in obtaining Equation (27) λ has been neglected compared to $\frac{[K(1-\beta)-1]}{\ell}$. Factoring, in turn, the denominator of (27) yields two roots, $s = \frac{K(1-\beta)-1}{\ell}$ and $s = 0$, respectively. This is possible if in the solution of the quadratic equation the term $\frac{(1-K)\lambda}{\ell}$ is neglected when compared to $\frac{[K(1-\beta)-1]^2}{\ell^2}$.

Thus, Equation (27) can be written as

$$\frac{N_1(s)}{H_1(s)} = \frac{s + \lambda}{s(s - \frac{[K(1-\beta)-1]}{\ell})} . \tag{28}$$

It is seen here that for frequencies higher than one radian per second, the zero in the numerator of Equation (28) cancels with the pole at the origin in the denominator and thus the source transfer function becomes

$$\frac{N_1(s)}{H_1(s)} = \frac{1}{s - \frac{[K(1-\beta)-1]}{\ell}} . \tag{29}$$

The transfer function $H_R(j\omega)$ is then

$$H_R(j\omega) = \frac{1}{j\omega - \frac{[K(1-\beta)-1]}{\ell}}, \qquad (30)$$

and the square modulus is

$$|H_R(j\omega)|^2 = \frac{1}{\omega^2 + \frac{[K(1-\beta)-1]^2}{\ell^2}}. \qquad (31)$$

For the critical case, the quantity $\frac{K(1-\beta)-1}{\ell}$ reduces to β/ℓ.

V. EXPERIMENTAL METHOD AND EQUIPMENT

The output of a nuclear reactor, namely, the neutron flux, when it is subject to analysis is initially translated into an electrical current by means of a system of instruments. This system usually consists of a neutron detecting device placed inside the reactor and a micro-microammeter. The nature of the neutron signal coming out of the micro-microammeter is such that is can be described as "noise". It is a response with random variation, which is a true characteristic of the microscopic behavior of the neutron flux inside the reactor. It is this noise that the present investigation is concerned with, and specifically, the analysis of this random signal with respect to different frequencies.

A. Derivation of the Experimental Power Spectra Definition

It is of interest, here, to show how the power spectral density can be measured experimentally. It will be shown that the power spectral density of a random signal in a given bandwidth of frequencies is proportional to the average of the mean square of the signal, evaluated at the corresponding mid-band frequency and divided by the bandwidth.

Considering a random function of time, f(t), extended infinitely along the axis, it has been shown (5, p. 58) that its mean square value is given by

$$\overline{x(t)^2} = \int_{-\infty}^{\infty} G(\omega)d\omega \qquad (32)$$

where, $G(\omega)$, is the power spectral density of the function. Also, the same mean square value evaluated at a particular frequency can be expressed as an average of the total power component of that frequency. Hence,

$$\overline{x(t)^2}\Big|_{\omega_o} = \frac{1}{T}\int_0^T x^2(t)\Big|_{\omega_o} dt = \int_{-\infty}^{\infty} G(\omega)d\omega \ . \qquad (33)$$

Limiting the frequency domain to the positive range, Equation (33) becomes

$$\frac{1}{T}\int_0^T x^2(t)\Big|_{\omega_o} dt = 2\int_0^{\infty} G(\omega)d\omega \ . \qquad (34)$$

If the particular frequency ω_o is defined as the mid-band frequency of a bandwidth limited by the frequencies ω_1 and ω_2 on each side, and assume that the power spectrum is constant inside that bandwidth and zero outside of it, expression (34) becomes

$$\frac{1}{T}\int x^2(t)\Big|_{\omega_o} dt \propto \int_{\omega_1}^{\omega_2} G(\omega)d\omega \propto G(\omega)\Big|_{\omega_1}^{\omega_2} \ . \qquad (35)$$

The right side of expression (35) is then approximated by $G(\omega_o)\Delta\omega$ with the assumption that the two limits of the frequency bandwidth, ω_1 and ω_2 are very near the

mid-band ω_o.

Thus

$$\frac{1}{T}\int_0^T x^2(t)\Big|_{\omega_o} dt \propto G(\omega)\Delta\omega, \tag{36}$$

or

$$G(\omega_o) \propto \frac{1}{\Delta\omega T}\int_0^T x^2(t)\Big|_{\omega_o} dt. \tag{37}$$

The right hand side of expression (37) can be determined experimentally by means of an analog computer. A band-pass filter, a square multiplier, and a summing circuit are used for this purpose.

B. Equipment

Experimentally, the main interest is to reduce the detected signal to the desired power spectra which will provide, in turn, information about the reactor transfer function. The technique makes use of an analog computer and, in summary, makes use of the following equipment:

1. A gamma-compensated Westinghouse ionization chamber
2. A Keithley pre-amplifier electrometer model 610
3. A Donner analog computer model 3500
4. A Krohn-Hite model 330-A band-pass filter
5. The reactor was the Iowa State University UTR-10[1], a modified commercial version of the Argonaut reactor developed at Argonne National Laboratory. Its core consists of two 5 in. by 20 in. by 24 in.

---

[1]A product of Advanced Technology Laboratories, a Division of American Standard, Mountain View, California.

subcores, each containing six fuel elements which are surrounded by graphite and cooled by deionized light water. A thermal column 4 ft. by 5 ft. by 5 ft. long is provided. Removable stringers are provided through openings in the top shield closures. Also, an access port to the mid-plane of the south fuel region is available after removing the central graphite stringer in the thermal column. Figure 2 shows the locations of stringer positions used in this investigation.

C. Signal Conditioning

The instrumentation used for conditioning the signal is shown in Figure 3 and is similar to the one used by Leribaux (6). The random signal was detected with a maximum magnitude of approximately thirty millivolts peak to peak, and was initially fed to an operational amplifier of the analog computer which had an amplification of one hundred. At this point the DC level of the signal, which is of no immediate interest, was eliminated by adding a bucking DC voltage of equal magnitude and of opposite sign to it. The amplified and DC filtered signal was then fed directly to the band-pass filter for frequency selection. The filter was used with the narrowest possible passing band; this was obtained by setting the high and low cut-off frequencies equal. The filtered signal, in turn, was again fed into an operational amplifier for additional amplification and DC filtering. An effort was made, at this point, to obtain a magnitude of about one hundred volts peak to peak since a calibration curve of the squaring

Figure 2. Plan view of UTR-10 showing important features and detector locations

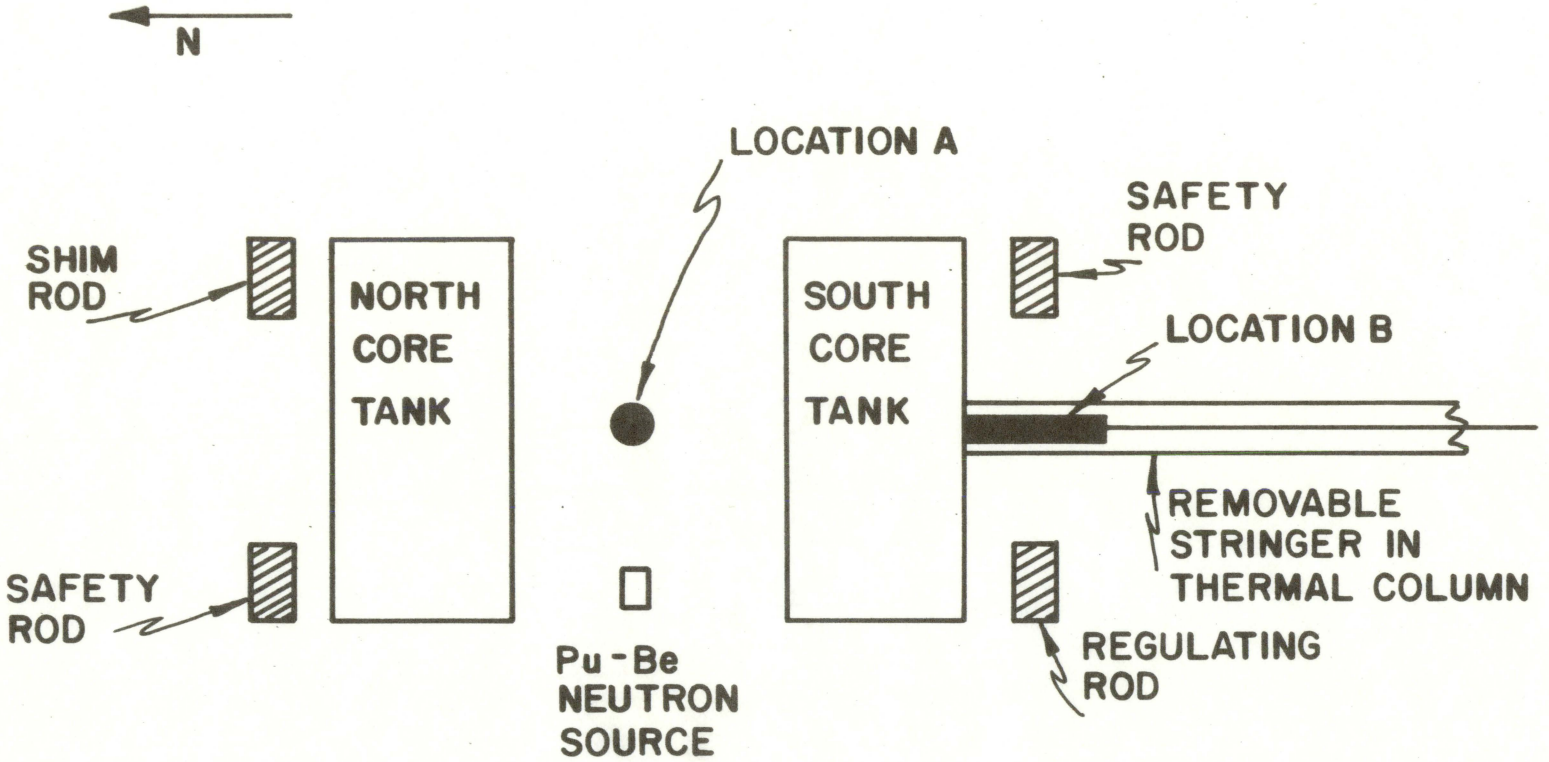
N
LOCATION A
SAFETY
ROD
SHIM
ROD
NORTH
CORE
TANK
SOUTH
CORE
TANK
LOCATION B
REMOVABLE
STRINGER IN
THERMAL COLUMN
SAFETY
ROD
REGULATING
ROD
Pu-Be
NEUTRON
SOURCE

Figure 3. Simplified diagram of instrumentation used

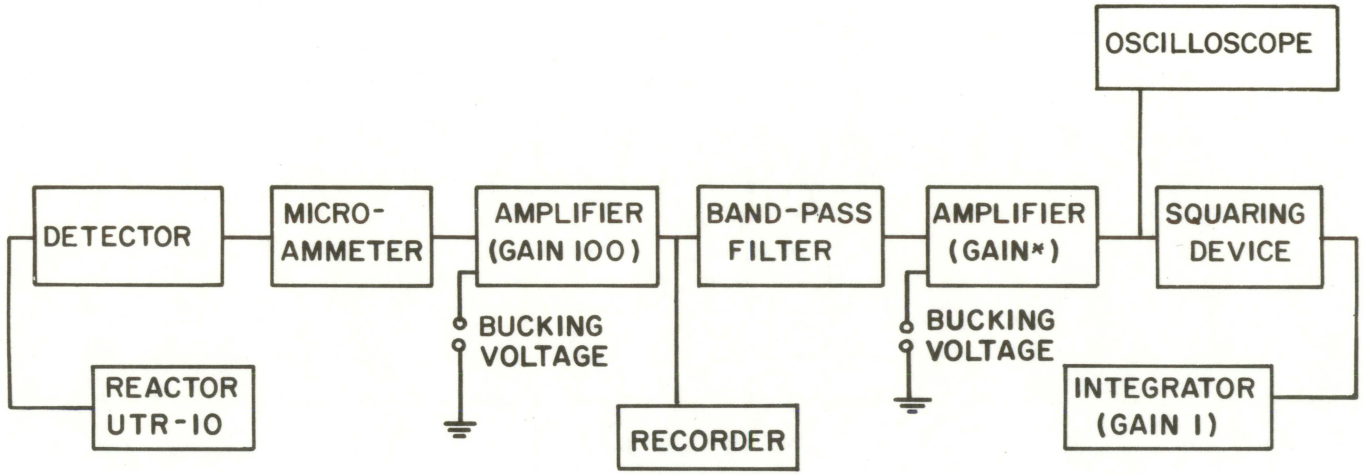
OSCILLOSCOPE
DETECTOR
MICRO-
AMMETER
AMPLIFIER
(GAIN 100)
BAND-PASS
FILTER
AMPLIFIER
(GAIN*)
SQUARING
DEVICE
BUCKING
VOLTAGE
BUCKING
VOLTAGE
REACTOR
UTR-10
RECORDER
INTEGRATOR
(GAIN 1)

* VARIED

device (Appendix C) showed the best accuracy for inputs of approximately this magnitude. The DC component of the signal was again bucked out, for any DC component present would be amplified, squared and integrated along with the other frequency components introducing an error into the measured power spectral density. Actually, the DC level was kept within 0.5 volts on the average. When this value is squared it becomes 0.0025 volts and after integration for 120 sec (with no integrator gain) it yields an error of 0.3 volts. This corresponds to a relative error of 0.6 per cent when compared to the integrated voltages obtained throughout the measurements.

Leribaux (6) suggested that before the bucking voltage is applied to the input of the operational amplifier, the band-pass filter should be shorted since the DC level is independent of the input to the band-pass filter. When this method is followed, however, special precautions must be taken for the reason that the band-pass filter consists mainly of DC coupled amplifiers with large capacitors and, thus, with very long time constants. A static input, such as the shorting of the input, produces transients of considerable magnitude which take some time to die out. Thus, it is advisable after shorting out the input of the band-pass filter to wait for at least fifteen seconds before taking a measurement.

The signal is then squared by means of a Donner Quarter Square Multiplier, model 3731. As was mentioned previously for minimum error the input to the squaring device should have a magnitude of about a hundred volts. The calibration curve for the square multiplier (see Appendix C) indicates an error of 0.25 per cent for inputs of this magnitude. When the signal, however, was analyzed with respect to high frequencies, for example above 100 cycles per second, it was impossible to maintain large magnitudes without introducing large drifts into the signal from the band-pass filter. Consequently, a compromise was made and sometimes the input to the squarer was as small as thirty volts peak to peak. The minimum error for squaring such a magnitude, with the squaring device used, is shown from the calibration curve to be 2.2 per cent.

D. Signal Recording

The recording of the signal requires integration for a period of time, averaging the sum over the bandwidth, and normalizing the final result to the variable gain used in the second amplification stage.

It was mentioned previously that the present measurements include noise contributions from the driving neutron source and the instrumentation itself. The final result then should be corrected with respect to these noise contributions. However, Leribaux (6) showed that these

noise contributions are uncorrelated or "white" up to high frequencies beyond the span which is of interest in the present investigation.

The squared signal was integrated for a period of time, usually for about two minutes. Longer integration time would yield better accuracy; however, in the present case a compromise had to be made for there was a time limitation on the operation of the reactor.

The output of the integrator was then averaged over the bandwidth, and thus, the signal was reduced to the desired power spectral density. Since the gain of the second amplifier was varied for different frequencies, the final magnitude of the power spectral density was normalized using the factor $(\frac{a_i}{a})$, where a_i was the variable gain and a_1 was the gain chosen for a standard. In this way the power spectral density was obtained for a range of frequencies from 0.1 cps up to 100 cps.

Since the data obtained here are the co-ordinates of a frequency response curve describing the characteristic transfer function of the reactor, the determination of the exact corner frequency had to be made by fitting the data by the method of least squares into the equation describing the transfer function of the reactor. One of the parameters that was varied for a best fit was the corner frequency.

The least square fit of the expression $A + B|h_r(j\omega)|^2$

was programed into the language of the IBM 7074 computer and used for the determination of the corner frequency. The program used is given in Appendix B.

Figure 4. Simplified diagram of instrumentation used for the special detecting technique

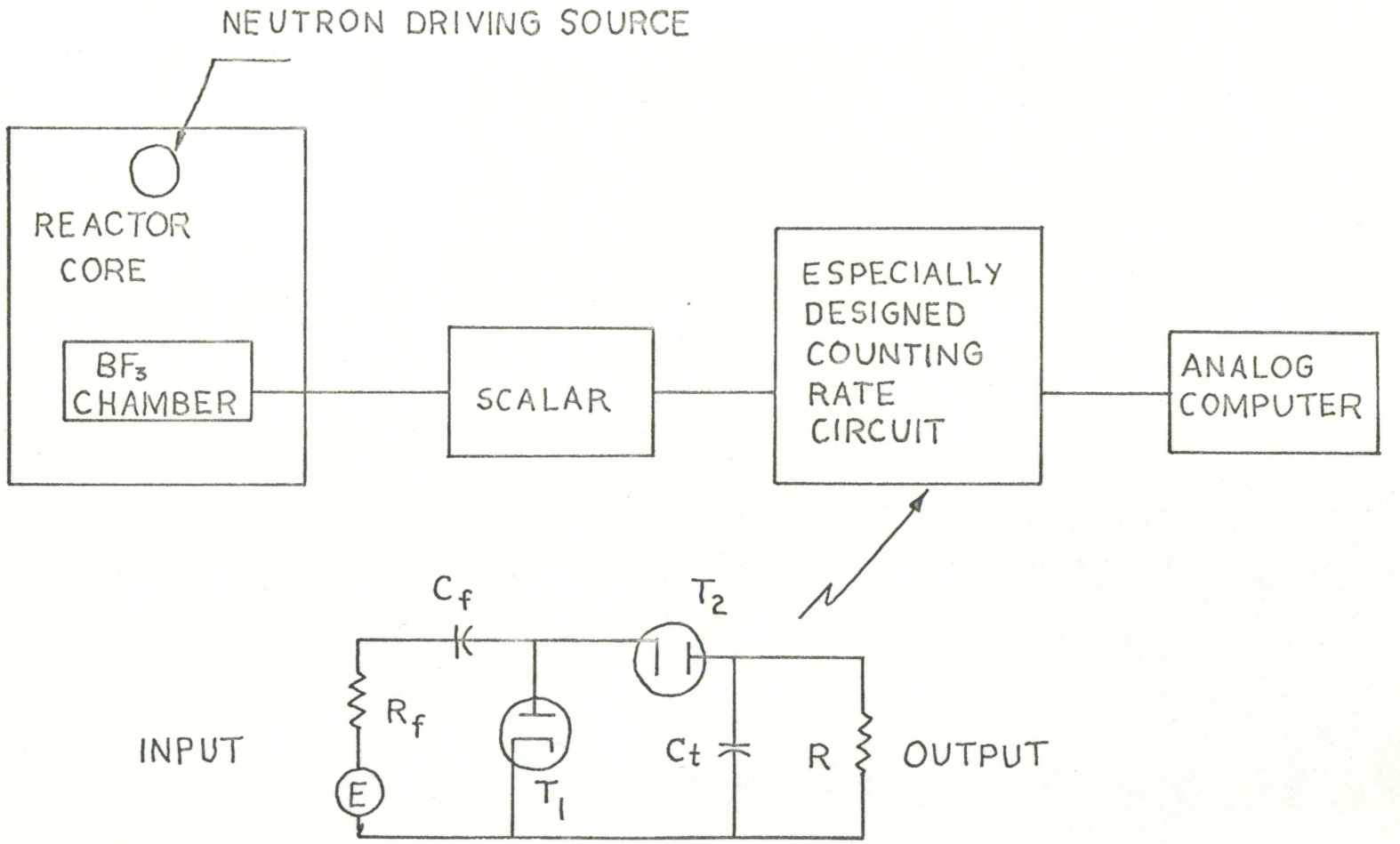
NEUTRON DRIVING SOURCE
REACTOR CORE
BF_3 CHAMBER
SCALAR
ESPECIALLY DESIGNED COUNTING RATE CIRCUIT
ANALOG COMPUTER
C_f
T_2
R_f
INPUT
E
T_1
C_t
R
OUTPUT

E. Investigation of a Special Low Neutron Flux Detecting Technique

During the initial stage of the present study, a special technique for detecting low neutron fluxes from a subcritical reactor was investigated.

A BF_3 detector was used in series with a scalar and a counting rate circuit as shown in Figure 4. The counting rate circuit was borrowed from Price (8) and works primarily on a counting rate to voltage linear relationship. It consists basically of an integrating circuit with integrates the incoming pulses from the BF_3 detector and, in turn, displays the result on an arbitary time scale. A tank capacitor at the input of the circuit absorbs the incoming pulses, and when the voltage across it builds up to an equilibrium value, at which the rate of loss of change through the shunt resistor equals the rate of input of the charge by the pulses, it feeds the collested voltage to the integrator through a flow directing system of diodes. Limitations imposed on the values of the parameters insure that sufficient time elapses for equilibrium to be reached before the next pulse arrives, and that negligible charge remains on the tank capacitor.

A sample of the signal coming out of the described special detecting apparatus is shown in Figure 5.

Figure 5. Random signal sample obtained with the special detecting technique

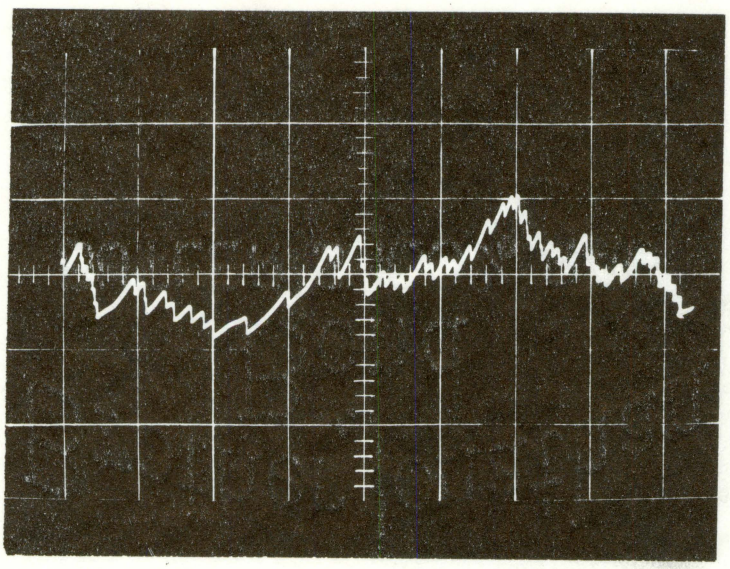

VI. RESULTS

A. Discussions of Results Obtained with the Use of an Ionization Chamber for Detecting the Neutron Flux.

An inoization chamber was placed at two different locations inside the reactor to detect the neutron flux fluctuations. The two locations are shown in Figure 2. The corner frequencies obtained, with both safety rods completely withdrawn and with the regulating and shim rods withdrawn to make the reactor critical, are summarized in Table 1.

Table 1. Corner frequency comparison

Chamber location	Safety rods No.1 and No.2	Shim Rod	Regulating Rod	Corner frequency β/ℓ (sec^{-1})
A	up	13.1"	4.6"	28.3
B	up	7 "	7 "	66.0

As can be seen the ratio β/ℓ is quite different at the two locations. The same results can be illustrated by comparing the corner frequencies of the corresponding Bode plots in Figure 6. The power spectral density for the reactor critical and for chamber location A is compared to the one obtained by Badgley (1) in Figure 7.

With the reactor in the subcritical state, all rods in and water at operating level, the power spectral density obtained for chamber location A is shown in Figure 8.

Figure 6. Bode plots for the reactor critical and for two different detector locations

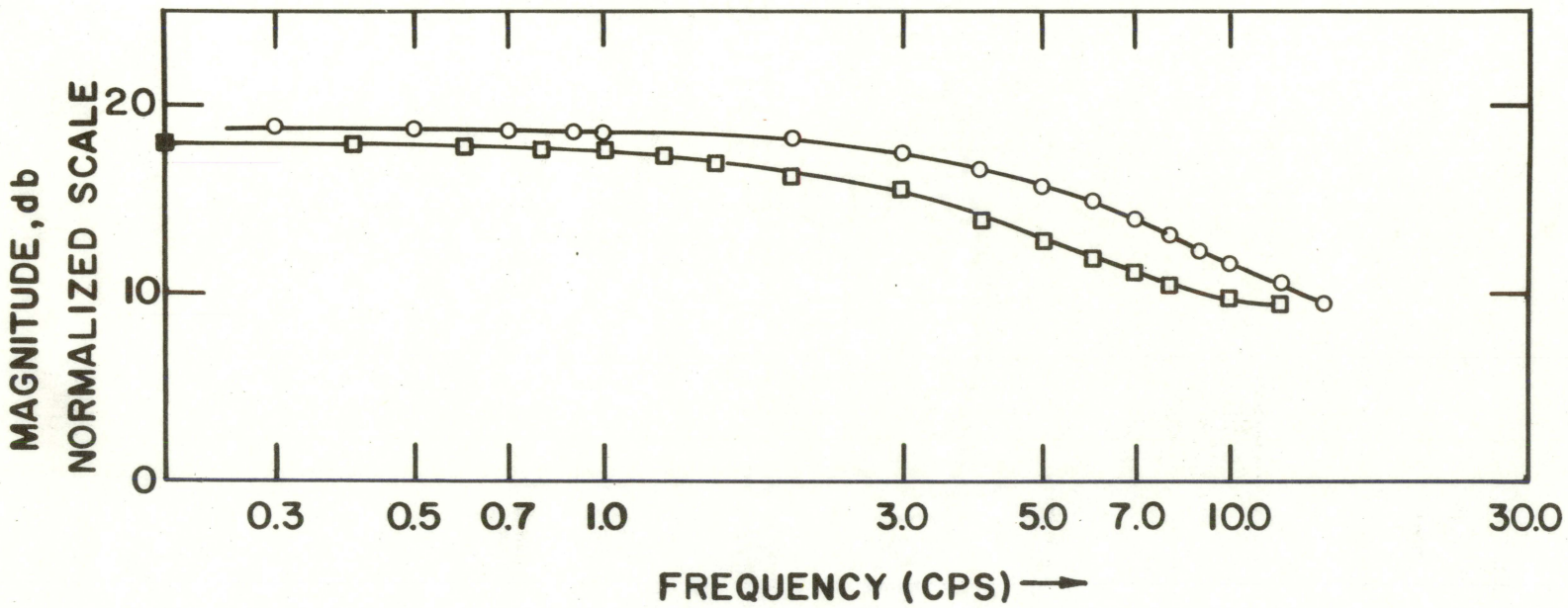

LEGEND: □ CHAMBER LOCATION A
○ CHAMBER LOCATION B

Figure 7. Power spectral density for the reactor critical and for chamber location A, compared to the one obtained by Badgley

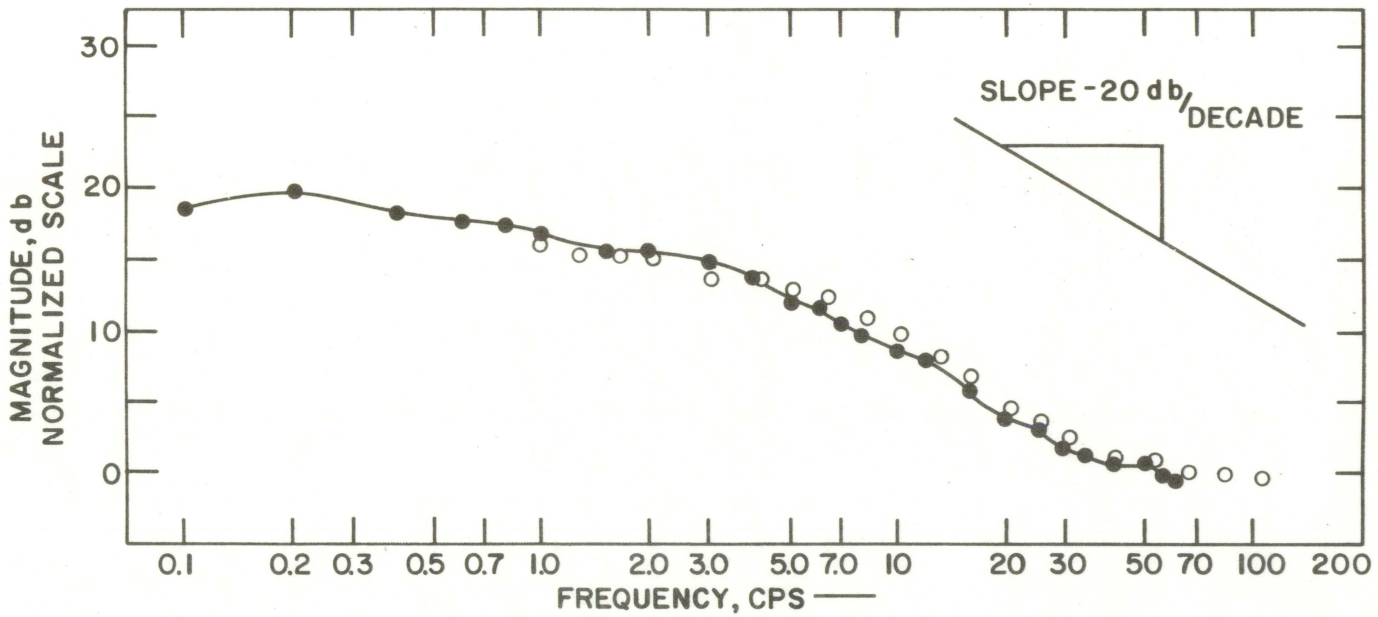

LEGEND: ● EXPERIMENTAL RESULTS OF PRESENT STUDY

○ EXPERIMENTAL RESULTS OF BADGLEY AND UHRIG (2)

Figure 8. Power spectral density for the reactor subcritical and for chamber location A

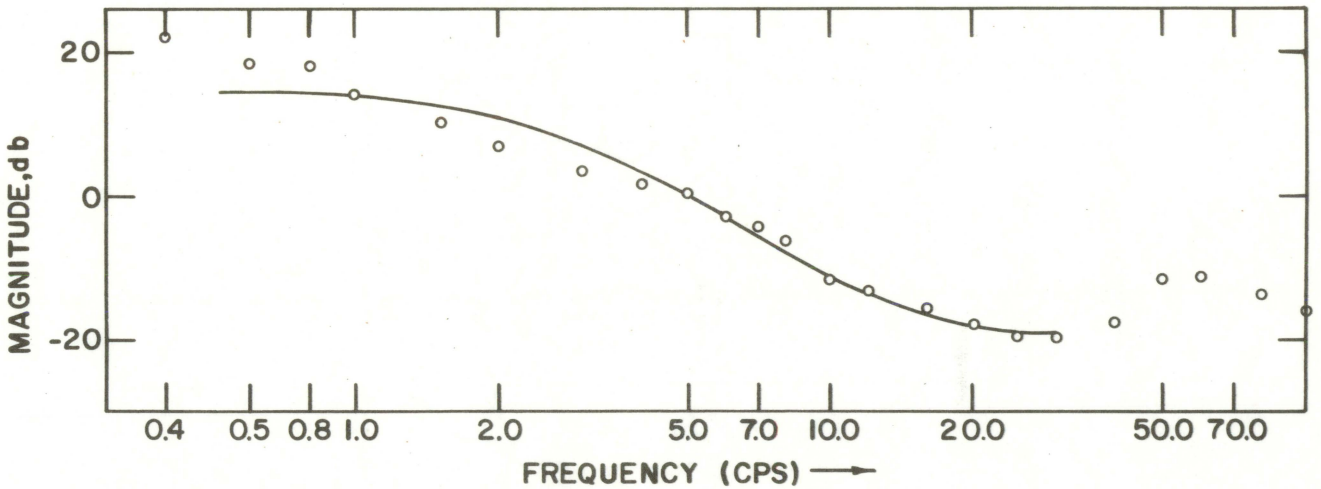
20
0
-20
MAGNITUDE, db
0.4
0.5
0.8
1.0
2.0
5.0
7.0
10.0
20.0
50.0
70.0
FREQUENCY (CPS) →
LEGEND: — THEORETICAL
o EXPERIMENTAL

Also, Figure 9 compares the corner frequencies for the reactor critical and subcritical for chamber location A. Table 2 summarizes the above result with respect to Keff (effective reproduction constant). Keff was calculated from the quantity, $\left[\frac{1-Keff(1-\beta)}{\ell}\right]$, by substituting the values .0070 for β and 247μsec for ℓ, the later obtained from the measurements taken at position A.

Table 2. Reactivity comparison

Chamber Location	Safety Rods No. 1 and No. 2	Shim Rod	Regulating Rod	Water Level	Keff*
A	up	13.1	4.6"	operating level	1.00000
A	up	down	down	operating level	0.99813

* At a temperature of 87° F

A run was also made with the reactor subcritical for chamber location B. However, the results were rather meaningless because the ionization chamber could not detect the extremely low neutron flux for this case. The power spectral density for this run is shown in figure 10.

B. Results Obtained with the Special Detecting Technique

Here, the special detecting technique which has been described in section V(E) was used for the determination of the shutdown reactivity margin of the reactor. Two cases were investigated, both with the reactor in a sub-critical state. Run 1 measured the power spectral density of the reactor with all rods in and the water in the core tanks at operating level. The result is shown in Figure II where the obtained power spectral density is compared with the frequency response of the detecting instrumentation. As it can be seen there is no difference between the two curves, which is an indication that the "white" noise of the instrumentation screens the reactor noise and, thereby, making its detection impossible.

On the other hand, run 2, which involved the determination of the power spectral density of the reactor with no water in the core tanks and all rods in, yielded a Bode plot with a corner frequency of about 250 cps. This is shown in figure 12. This corner frequency corresponds to a Keff of approximately .6163 which is in close agreement with the expected value.

Finally, the data which described all of the above Bode plots are tabulated in Appendix A.

Figure 9. Comparison of power spectral densities for the reactor critical and subcritical

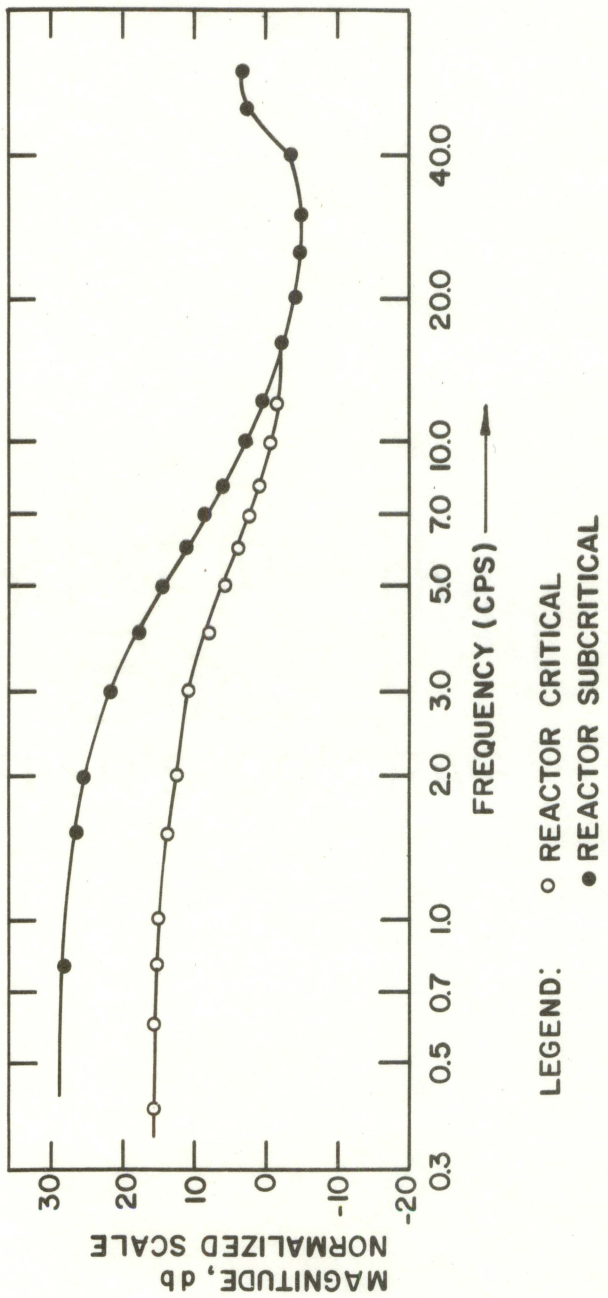
MAGNITUDE, db
NORMALIZED SCALE
30
20
10
0
-10
-20
0.3
0.5
0.7
1.0
2.0
3.0
5.0
7.0
10.0
20.0
40.0
FREQUENCY (CPS)
LEGEND:
○ REACTOR CRITICAL
● REACTOR SUBCRITICAL

Figure 10. Power spectral density for the reactor subcritical and for chamber location B

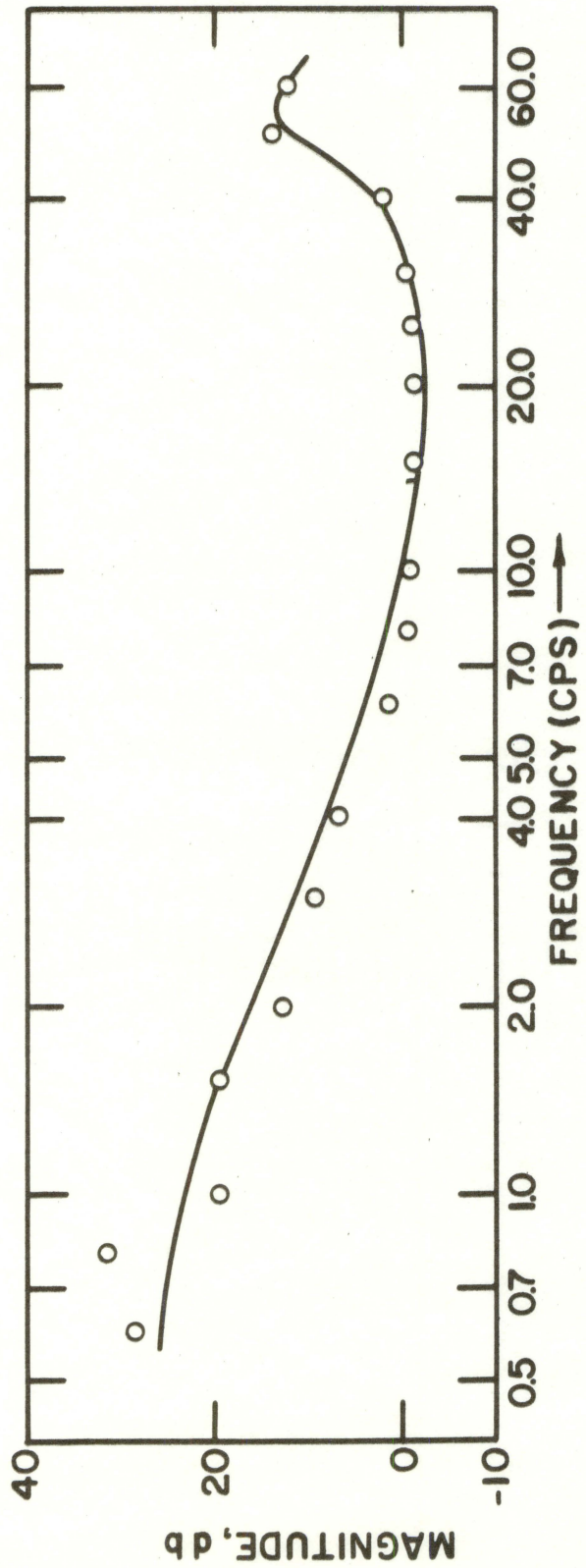
MAGNITUDE, db
40
20
0
-10
0.5
0.7
1.0
2.0
4.0
5.0
7.0
10.0
20.0
40.0
60.0
FREQUENCY (CPS)

Figure 11. Power spectral density of the reactor with all rods in and the water at operating level, measured by the special detecting technique

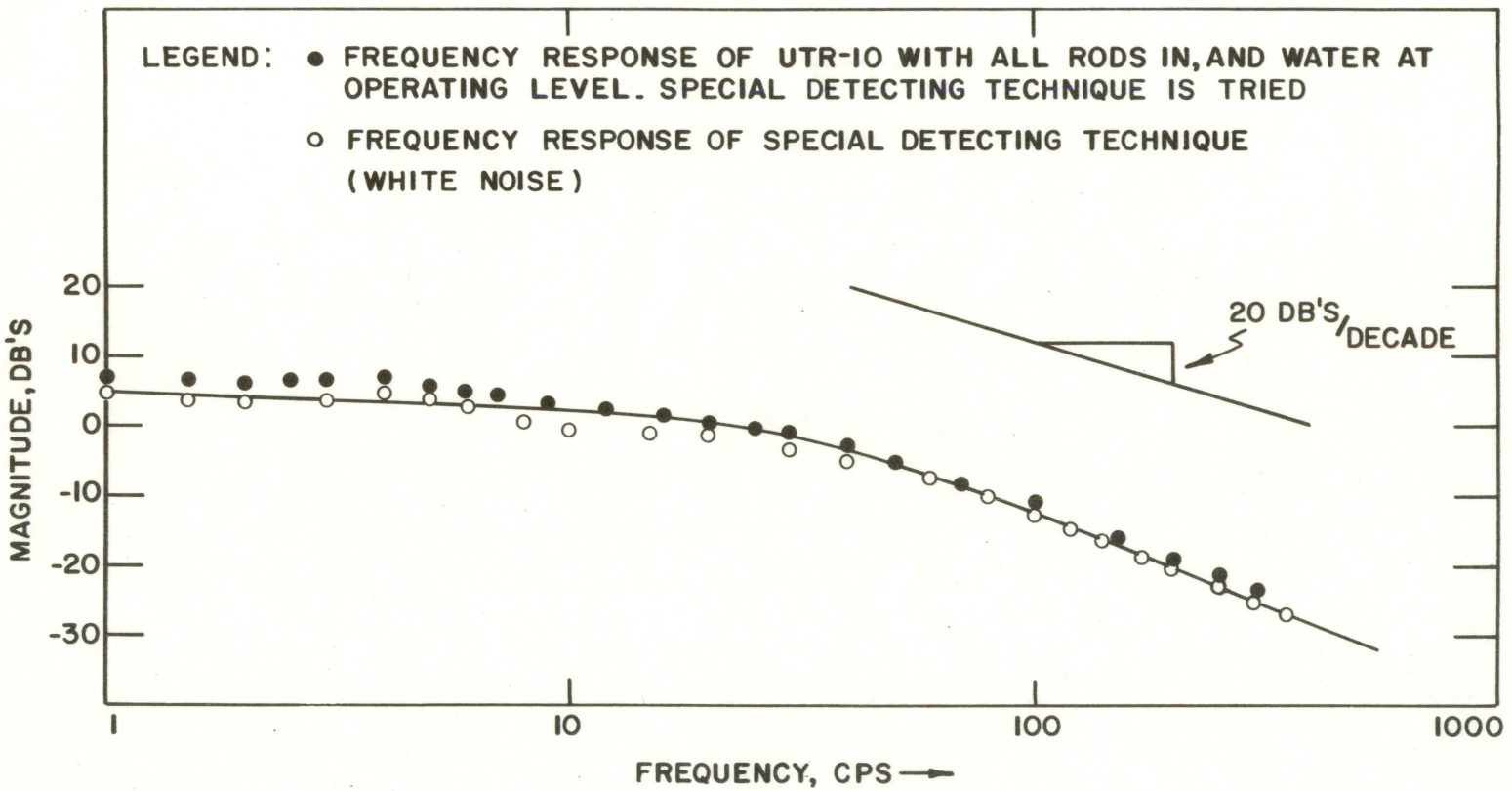
LEGEND: ● FREQUENCY RESPONSE OF UTR-10 WITH ALL RODS IN, AND WATER AT OPERATING LEVEL. SPECIAL DETECTING TECHNIQUE IS TRIED
○ FREQUENCY RESPONSE OF SPECIAL DETECTING TECHNIQUE (WHITE NOISE)
20 DB'S/DECADE
MAGNITUDE, DB'S
20
10
0
-10
-20
-30
1
10
100
1000
FREQUENCY, CPS

Figure 12. Power spectral density of the reactor with no water in the core tanks and all rods in, measured by the special detecting technique

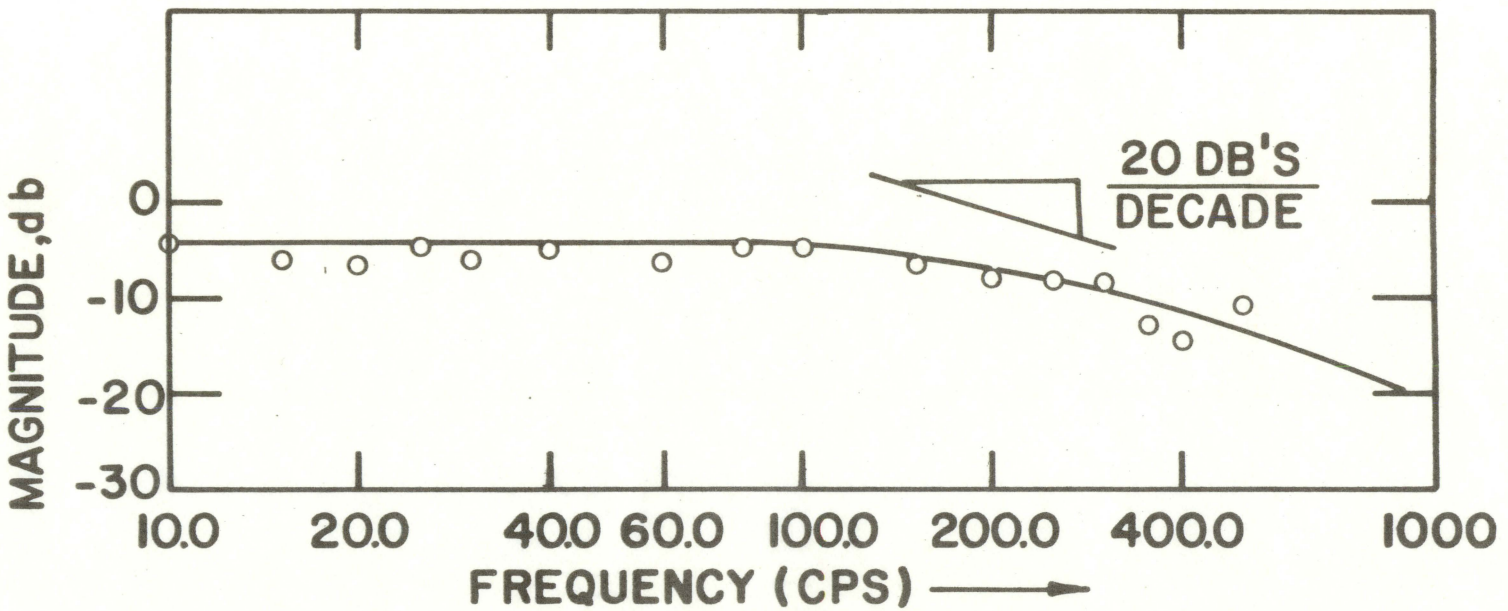

NOTE: CORRECTION ALREADY MADE FOR "WHITE" NOISE

VII. CONCLUSIONS

Within the scope of this investigation the following conclusions are justified.

1. The power spectral densities exhibit different characteristics at the two locations inside the reactor used in this study. Thus, it appears spatial effects should be included in a complete mathematical description of the system.
2. The power spectral density of the neutron fluctuations in a subcritical reactor is a function of the degree of departure of the system from criticality.
3. The results of this investigation indicate that it is feasible to measure the shutdown margin of a reactor with random noise techniques.
4. The assumptions made in obtaining the proportionality between the analytical power spectral density and the experimental one, call for a perfect band-pass filter. That is, they require a band-pass filter which can provide absolute frequency discrimination outside the limits of the band in question. During the measurements, though, the presence of low frequency drifts within most frequency bandwidths indicated that the band-pass filter presents a drawback in the use of power spectral density for shutdown reactivity measurements.

5. Finally, the use of ionization chambers for detecting low neutron fluxes is limited. High sensitivity, low noise equipment must be used if good results are to be obtained.

VIII. SUGGESTIONS FOR FUTURE WORK

The suggestions concerning some possible future investigations on power spectral density measurements for subcritical reactors are many in number. They are limited, however, by the instrumentation available at the present time. Thus, the following suggestions are only those investigations which do not require any extra equipment than the available.

1. For analytical type of work, it is suggested a study be made to obtain a more accurate theoretical model to describe the kinetic behavior of the reactor. Along with its accuracy, the model should be flexible enough to enable the investigator to apply a simple interpretation of the experimental results.
2. As an experimental study, it is suggested an investigation be made for the design of a more accurate technique in order to be able to detect low neutron fluxes coming from subcritical assemblies. It is suggested the study be a continuation of the already presented investigation included in the present work.

3. The availability of such a detecting technique leads, finally to the suggestion of determining more accurately the shutdown reactivity margin of the UTR-10 reactor, which is believed to be of great use to the operator.

IX. LITERATURE CITED

1. Badgley, R. W. Power spectral density measurements on the University of Florida Training Reactor operating in the subcritical region. Unpublished M.S. thesis. Library, University of Florida. Gainesville, Florida. 1962.

2. Badgley, R. W. and Uhrig, R. E. Power-spectral-density measurements in a subcritical reactor. Nuclear Science and Engineering 19: 158-168. 1964.

3. Danofsky, R. A. Random noise analysis in the Iowa State University UTR-10 reactor. Unpublished Ph.D. thesis. Library, Iowa State University of Science and Technology. Ames, Iowa. 1963.

4. Griffin, C. W. and Lundholm, J. G. Measurements of the SRE and KEWB prompt neutron lifetime using random noise and reactor oscillation techniques. U. S. Atomic Energy Commission Report NAA-SR-3765 [Atomincs International, Canoga Park, California]. October 15, 1959.

5. Lee, Y. W. Statistical theory of communications. John Wiley and Sons. New York. 1960.

6. Leribaux, H. R. Stochastic processes in coupled nuclear reactor cores. Unpublished Ph.D. thesis. Library, Iowa State University of Science and Technology. Ames, Iowa. 1963.

7. Moore, M. N. The determination of reactor transfer functions from measurements at steady operation. Nuclear Science and Engineering 3: 387-394. 1958.

8. Price, W. J. Nuclear radiation detection. McGraw-Hill Book Company, Inc. New York. 1958.

9. Rice, S. O. Mathematical analysis of Random Noise. Bell Systems Technical Journal 23: 284. 1944.

10. Schultz, M. A. Shutdown reactivity measurements using noise techniques. Unpublished paper presented at the Symposium on Noise Analysis in Nuclear Systems, Gainesville, Florida, University of Florida, 1963. Multilithered. Department of Nuclear Engineering, University of Florida. Gainesville, Florida. 1964.

11. Schuster, A. Acta. Math. 55: 117-258. 1930.

12. Thie, J. A. Operating information from reactor noise. Nucleonisc 21, No. 3: 72. March 1963.

13. Thie, J. A. Reactor noise. Rowman and Littlefield, Inc. New York. 1963.

14. Uhrig, R. E. Random variations of neutron density in a subcritical assembly. American Nuclear Soc. Trans. 4, No. 1: 85. 1961.

X. ACKNOWLEDGEMENTS

The author wishes to express his gratitude to his major professor, Dr. Richard Danofsky, Assistant professor in Nuclear Engineering at Iowa State University. His advise and keen personal interest for the present investigation are highly appreciated.

A special appreciation is expressed by the author to his father whose financial support made this educational experience possible.

It is also a pleasure to express appreciation to Dr. Howard Jespersen and Mr. Tatsuhiko Ando for their contribution in writing the program for the IBM-7074 computer.

XI. APPENDIX A

A. Tabulation of Experimental Data

Table 3. Power spectra data for reactor critical, location A

Frequency (CPS)	Experimental Magnitude, db	Theoretical Magnitude, db
0.1	18.30	17.94
0.2	19.73	17.93
0.4	18.31	17.86
0.6	17.72	17.76
0.8	17.32	17.61
1.0	16.53	17.44
1.5	15.41	16.86
2.0	15.45	16.15
3.0	14.60	14.60
4.0	13.70	13.15
5.0	12.05	11.94
6.0	11.54	10.99
7.0	10.34	10.26
8.0	9.75	9.69
10.0	8.90	8.91
12.0	7.94	8.42

Table 4. Power spectra data for reactor critical, location B.

Frequency (cps)	Experimental Magnitude, db	Theoretical Magnitude, db
0.3	13.24	12.49
0.5	13.33	12.46
0.7	13.45	12.43
0.9	11.48	12.39
1.0	12.50	12.37
2.0	10.87	12.01
3.0	11.21	11.44
4.0	10.26	10.72
5.0	9.57	9.90
6.0	8.85	9.04
7.0	8.08	8.18
8.0	7.60	7.35
9.0	6.77	6.56
10.0	6.03	5.83
12.0	4.78	4.55
14.0	3.31	3.52
16.0		

Table 5. Power spectra data for reactor subcritical, location A.

Frequency (cps)	Experimental Magnitude, db	Theoretical Magnitude, db
0.8	18.08	13.09
1.0	14.07	12.77
1.5	10.30	11.68
2.0	6.82	10.28
3.0	3.64	6.88
4.0	1.82	3.22
5.0	0.56	0.25
6.0	- 3.33	- 3.32
7.0	- 4.26	- 5.92
8.0	- 6.12	- 8.08
10.0	-11.85	-11.32
12.0	-13.00	-13.52
16.0	-15.48	-16.13
20.0	-17.82	-17.52
25.0	-12.50	-18.47
30.0	-12.58	-19.02

Table 6. Power spectra data for reactor subcritical, location B

Frequency (cps)	Experimental Magnitude, db
0.6	28.80
0.8	31.56
1.0	19.66
1.5	19.70
2.0	12.64
3.0	9.35
4.0	6.52
6.0	1.40
8.0	- 0.40
10.0	- 0.81
15.0	- 1.11
20.0	- 1.38
25.0	- 1.12
30.0	- 0.40
40.0	2.00
50.0	13.93
60.0	12.34

Table 7. Power spectra data for reactor subcritical, no water in core tanks, all rods in.

Frequency (cps)	Experimental Magnitude, db	Theoretical Magnitude, db
8.0	- 3.87	- 3.99
10.0	- 4.54	- 4.00
25.0	- 4.88	- 4.09
40.0	- 4.88	- 4.27
80.0	- 4.80	- 5.04
100.0	- 5.00	- 5.56
150.0	- 6.80	- 7.02
200.0	- 8.00	- 8.46
250.0	- 8.30	- 9.72
300.0	- 8.40	-10.75
350.0	-13.00	-11.58
400.0	-14.30	-12.23

XII. APPENDIX B

A. Fortran Statements

Power spectral density function

```
      DIMENSION ALPHA (50), W(200), Y(200), X(200)
15    READ INPUT TAPE 1, 10, ID, N, M
      ID1 = ID1
      M = M
      Z = N
      N = NUMBER OF POINTS, M = NUMBER OF ALPHAS
10    FORMAT (I10, I5, I3)
      READ INPUT TAPE 1, 11, (ALPHA (I), I = 1, M)
11    FORMAT (8F10.1)
      DO 12  J = 1, N
12    READ INPUT TAPE 1, 14, ID1, T, Y(I), W(I)
14    FORMAT (I10, I5, 2F10.0)
      WRITE OUTPUT TAPE 2, 13, ID
13    FORMAT (1H1, I10)
      DO 3  J = 1, M
      SUM X = 0
      SUM Y = 0
      SUM U = 0
      SUM V = 0
      DO 1  I = 1, N
      X(I) = 1.0/(ALPHA(J)**2 + W(I)**2)
      SUM X = SUM X + X(I)
      SUM U = SUM U + X(I)**2
      SUM Y = SUM Y + Y(I)
      SUM V = SUM V + X(I)*Y(I)
 1    CONTINUE
      B = (SUM V - SUM X*SUM Y/Z)/(SUM U - SUM X*SUM X/Z)
      A = SUM Y/Z - SUM X*B/Z
      SUM SQ = 0
      DO 2  I = 1, N
 2    SUM SQ = SUM SQ + (Y(I) - A - B* X(I)**2)
      WRITE OUTPUT TAPE 2, 20, ID, ALPHA(J), A, B, SUM SQ
20    FORMAT (1H0, I10, F10.2, 3E20.8)
      DO 31  I = 1, N
      YV = A + B*X(I)
      DV = Y(I) - YV
31    WRITE OUTPUT TAPE 2, 20, I, X(I), Y(I), YV, DV
 3    CONTINUE
      GO TO 15
      END
```

XIII. APPENDIX C

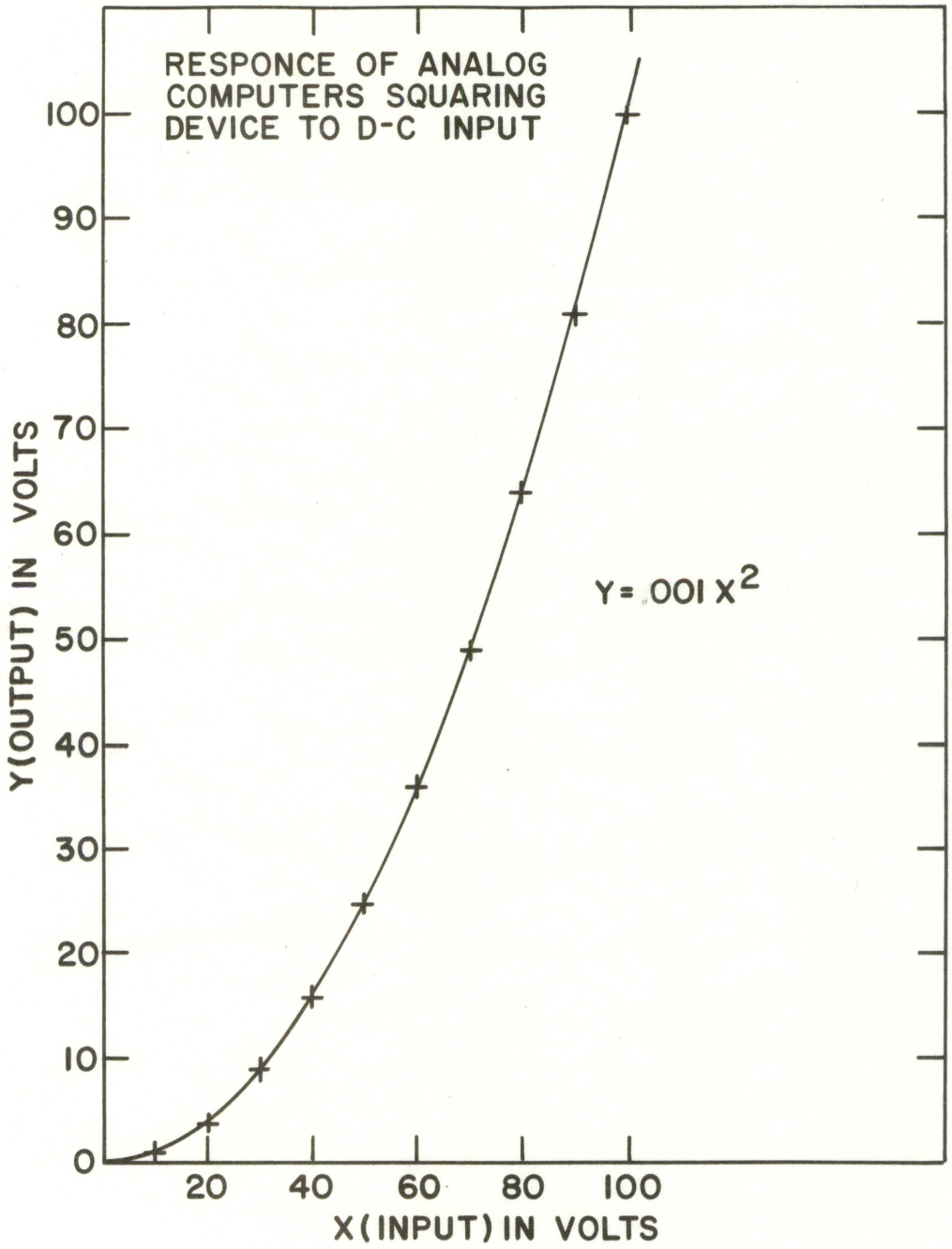

Figure 13. Calibration curve for square multiplier

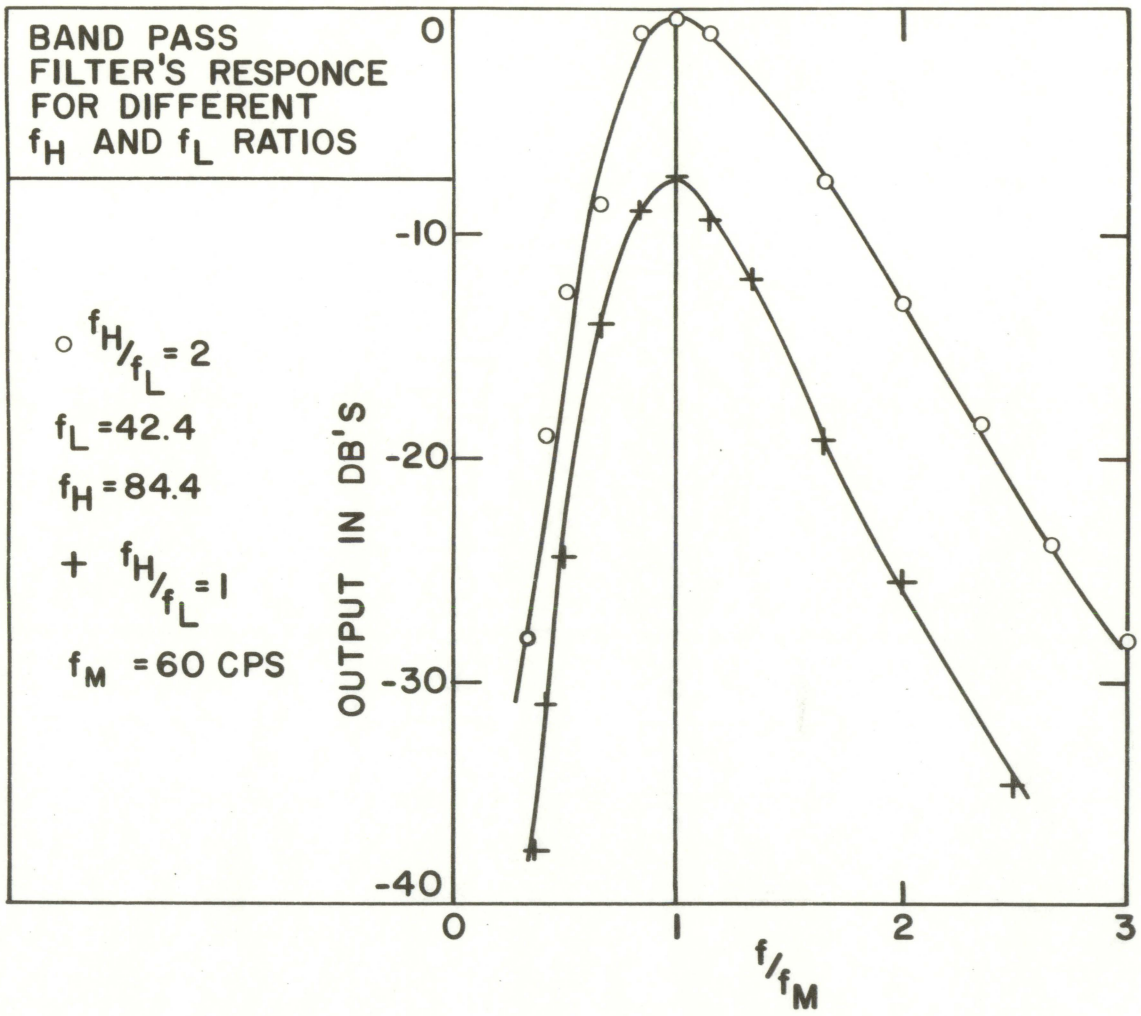

Figure 14. Calibration curve for the band-pass filter